SURFACE ORGANOMETALLIC CHEMISTRY OF WELL-DEFINED PALLADIUM ELECTRODES

Kim, Y.-G.; Chen, X.; Park, Y.-S.; Baricuatro, J.H.; Sanabria-Chinchilla, J.; Soriaga, M.P.*

Department of Chemistry. Texas A&M University. College Station, TX 77843. USA.
e-mail: Soriaga@Mail.Chem.TAMU.Edu

Received May 27, 2003. Accepted in Final Form June 4, 2003
Dedicated to Professor Dr. A.J. Arvia on occasion of his 75th Anniversary

Abstract

Experimental studies, based upon a combination of electrochemistry, scanning tunneling microscopy, and ultrahigh vacuum surface spectroscopy, onthe interaction of well-characterized palladium electrodes with a wide variety of organic compounds have served to establish the surface organometallic chemistry of this transition metal. The results from such investigations are showcased in the present review article.

Resumen

Estudios experimentales, basados en una combinación de electroquímica, microscopía de efecto túnel, y espectroscopía de superficie de ultra-alto vacío, en la interacción de electrodos bien caracterizados de paladio con una amplia variedad de compuestos orgánicos han servido para establecer la química organometálica superficial de este metal de transición. Los resultados de tales investigaciones son dados a conocer en el presente artículo de revisión.

Introduction

The chemical reactions that transpire when an electrocatalyst surface is exposed to organic molecules are of fundamental importance in electrochemical science and technology [1- 3]. Unfortunately, they are processes that are extremely difficult to describe quantitatively, especially at the atomic level. Early work on electrochemical adsorption at polycrystalline electrodes [4-7] was limited to traditional experimental and thermodynamic techniques [8-11] that yielded only the macroscopic properties of the interfacial systems under investigation. The need [12-16] for an atomic-level view of electrode reactions provided the impetus for later work that not only integrated non-traditional experimental techniques [17-24] but also explored the analogy between chemisorption and surface-chemical-bond formation [25-34]. Based upon earlier work of organic adsorption at polycrystalline Pt electrodes, a phenomenological classification of adsorption processes at the solution-metal electrode interface was proposed [35]. In this scheme, organic adsorbates were be classified into three groups: The first group was comprised of molecules, such as unsaturated and aromatic hydrocarbons, that bonded to the metal surface with or without bond rupture. The second included organic compounds that decomposed upon adsorption and yielded carbon monoxide-type surface intermediates; formic acid is a representative of this class. The third group was composed

of molecules that interact only weakly with the surface; saturated carboxylic acids would fall under this category. Such a classification scheme, however, is largely phenomenological and is centered solely on the behavior of the adsorbate; it does not take into account the chemical properties of the metal itself. It thus fails to predict that, on Pt, benzene would fall under the first category but, on Au, it lies in the third group. It cannot account for multiple modes of adsorption, and is deficient in the explanation as to why formic acid decomposes upon chemical adsorption.

It has been proposed [34] more recently that chemisorption be viewed in terms of established concepts [36, 37] of transition-metal coordination and organometallic chemistry. This approach, sometimes referred to as the "surface-cluster" analogy, recognizes the fact that chemisorption (surface coordination) must consider the chemical properties of *both* the adsorbate (ligand) and the electrode (metal center). In the surface-cluster analogy, the norm is that a commonality exists between an interfacial structure and a discrete molecule. Surface intermediates are thus modeled after well-characterized molecular or cluster complexes. As an example, non-dissociative adsorption of alkenes is described in terms of the bonding in Zeise's complex [36]. In the surface-cluster analogy, the above phenomenological classifications would be unnecessary since they are only manifestations of the gradation of the relative strengths of surface coordination between the metal surface and the solution constituents (solvent, electrolyte, and reagent). The strong surface activity of ethylene at Pt surfaces in aqueous media follows the aggressive reactivity of the same ligand with aqua-Pt complexes. Likewise, the weak adsorbability of saturated carboxylic acids is consistent with these ligands' comparatively weak coordinating properties. The chemisorption-induced decomposition of formic acid has its analogy in homogeneous coordination chemistry: *direct* reaction of HCOOH with a Pt complex leads to a decarbonylation reaction characterized by the formation of a Pt-CO bond [38]:

$$\mathrm{HCOOH + PtL_n{}^z \rightarrow Pt(CO)(H2O)L_n{}^z} \quad (1)$$

It is for this reason that Pt-formate complexes are synthesized by an *indirect* route that involves CO2 insertion into a metal-hydride bond.

A more comprehensive understanding of adsorption at electrode surfaces mandates the accumulation of a critical atomic-level database of prototypical interfacial systems. Technological [21-24] and theoretical [25-30] successes in the study of the physics and chemistry of the gas-solid interface have provided the impetus for the continued adaptation of proven surface-sensitive analytical methods in the investigation of the electrode-solution interface [17-20, 39-41]. Systematic studies of well-defined single-crystal electrode surfaces in conjunction with conventional and non-traditional techniques are no longer rare episodes. It is this type of studies at palladium electrodes that is the subject of the present review article.

Experimental

If chemisorption is to be described in terms of the making and breaking of metal-organic surface chemical bonds, experiments need to be conducted in such a manner that

ambiguities in data interpretation are minimized. Towards this objective, studies of *model* interfacial ensembles include the following experimental strategies [1,2,39]: (i) the use of compositionally pure and structurally well-characterized starting materials, (ii) the detailed structural and compositional analysis of important surface intermediates, and (iii) the identification and subsequent quantitative analysis of reaction product distributions. Investigations in electrochemical surface science are thus based upon the employment of single-crystal electrodes and surface-sensitive analytical methods.

The surface of a polycrystalline electrode is constituted by small domains of various crystallographic planes. Since different planes exhibit different properties, it is important to identify the processes associated with each domain, a task possible only if interfaces with uniform structural features are studied individually. The presence of unwanted species on the surface, even at low concentrations, can alter the chemistry of such interface. It is likewise imperative to utilize surfaces with uniform chemical compositions. The preparation *and* verification of clean and well-ordered electrode surfaces constitute critical steps in rigorous studies of molecular adsorption at the electrode-solution interface.

The low-index surface crystallographic faces, such as the (111), (110), and (100) planes of face-centered cubic crystals, have been widely used because of their low surface free energies, high symmetries, and relative stabilities. In addition, the resultant macroscopic behavior of smooth polycrystalline electrodes can usually be synthesized in terms of the individual properties of these three surface planes [42,43]; polycrystalline electrode surfaces have been modeled by the introduction of steps along the basal single-crystal planes [21,44-46].

Clean and Ordered Single-Crystal Surfaces

Two procedures were used in our work to prepare oriented monocrystalline surfaces. In the more common method, zone-refined single-crystal boules are oriented by the Laué back-reflection technique [47] and then cut along the desired crystal face. Metallographic polishing is subsequently done with successively finer grades of alumina or diamond paste in order to obtain a uniformly smooth surface. The oriented and polished single-crystal electrode is placed in a UHV chamber and subjected to near-melting temperatures in order to segregate bulk contaminants onto the surface. The surface impurities can either be oxidatively desorbed by high-temperature oxygenation or be sputtered away by Ar^+-ion bombardment; for parallelepiped single crystals, provisions must be made such that all six oriented faces can be subjected to ion bombardment. Atomic smoothness is achieved by a final high-temperature treatment of the clean, ion-bombarded surface. In accordance with standard surface science practice [21-24], surface analysis to ascertain interfacial structure and composition is always carried out prior to each experiment.

The second procedure is based on the fact that when a Pd wire (of purity greater than 99.995%) is melted in an oxygen-rich hydrogen flame and slowly cooled, a single-crystal bead approximately 3 mm in diameter is formed at the end of the wire [48-53]. Eight facets (0.2 mm in diameter), oriented in the (111) plane, and six smaller facets (0.08 mm in diameter), oriented in the (100) plane, appear on the single-crystal bead in octahedral and hexagonal arrangements, respectively. For voltammetric experiments, a

larger surface area is needed; hence, the facets are metallographically polished with the aid of laser diffraction to maintain the crystallographic orientation. Final treatment and/or regeneration of the clean and ordered surfaces consisted of flame annealing, slow cooling and immersion in ultrapure water [51-53].

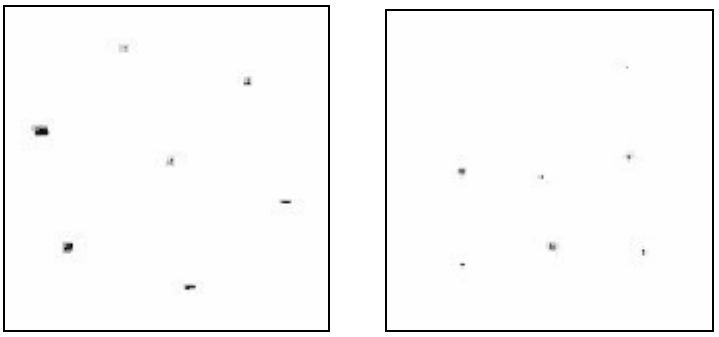

Figure 1*: Low-energy electron diffraction (LEED) pattern of UHV-prepared clean and well-ordered Pd(111)(left) and Pd(100)(right) surfaces. Electron beam energy = 60 eV; beam current = 2 μA.*

Interfacial Characterization

The cleanliness and single crystallinity of electrode surfaces cannot simply be assumed even if the preparative steps outlined above are followed. The interfacial characterization methods employed to date have been conveniently classified in terms of whether they are conducted under reaction conditions (*in situ*) or outside the electrochemical cell (*ex situ*).

In situ methods that have been employed in our studies include cyclic voltammetry of electrochemical (EC) adsorption/desorption reactions [49-50] and scanning tunneling microscopy (STM) [51-53]. EC-STM experiments were carried out with a Nanoscope E microscope (Digital Instruments, Santa Barbara, CA) equipped with a custom-built Kel-F electrochemical cell. The tunneling tips were prepared by electrochemically etching a tungsten wire; 0.25-mm in diameter, in 1 *M* KOH at 15 VAC. Functionally sharp STM tips are manifested when, at 800X-magnification, visual acuity of the tip is no longer attainable. The choice tips were then sealed with nail polish to minimize the faradaic current. Routine EC-STM images, atomically resolved, of the clean Pd(*hkl*) surfaces demonstrated the lack of contamination from the nail polish.

Ex situ methods are based upon the analysis of electrons, ions, molecules or atoms scattered/released from solid surfaces [21-24]. The shallow escape depths of these particles make their use most suitable for interfacial studies since the information they bear are characteristic only of the near-surface layers; on the other hand, the short mean-free paths necessitate a high vacuum environment. The major limitation is the possibility of structural and compositional changes upon removal of the electrode from solution (emersion) and transfer into the surface analysis chamber. Numerous studies have established that the compact layer remains largely unperturbed upon evacuation [54-56] unless the emersion layer contains feebly-bound noncondensed species. The following UHV-based methods were used in our investigations [39-41]: Low-energy electron

diffraction (LEED) for surface crystallography; Auger electron spectroscopy (AES) and X-ray photoelectron spectroscopy (XPS) for elemental analysis; Highresolution electron energy loss spectroscopy (HREELS) for surface vibrational spectroscopy; and temperature-programmed desorption (TPD) for adsorption energetics.

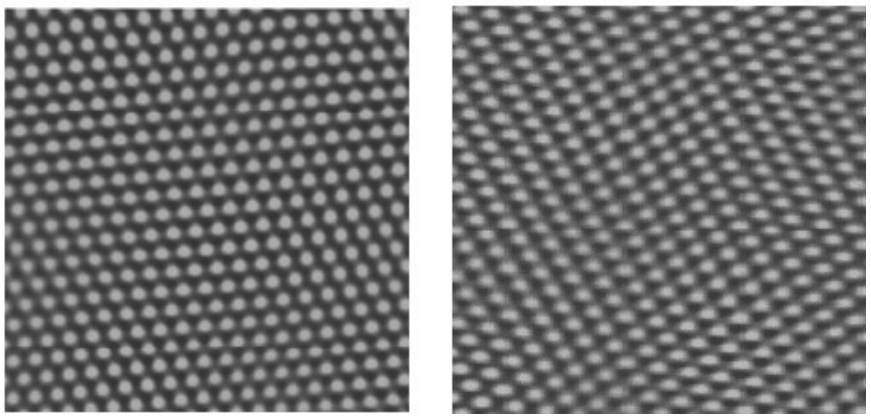

Figure 2*: Electrochemical scanning tunneling microscope (EC-STM) images of flame-annealed clean and well-ordered Pd(111) (left) and Pd(100) (right) surfaces in 0.05 M* H_2SO_4*. Bias voltage = 200 mV. Tunneling current = 20 nA.*

Typical LEED patterns, EC-STM images, and AES spectra for clean and ordered Pd(*hkl*) electrode surfaces are shown, respectively, in Figures 1, 2 and 3.

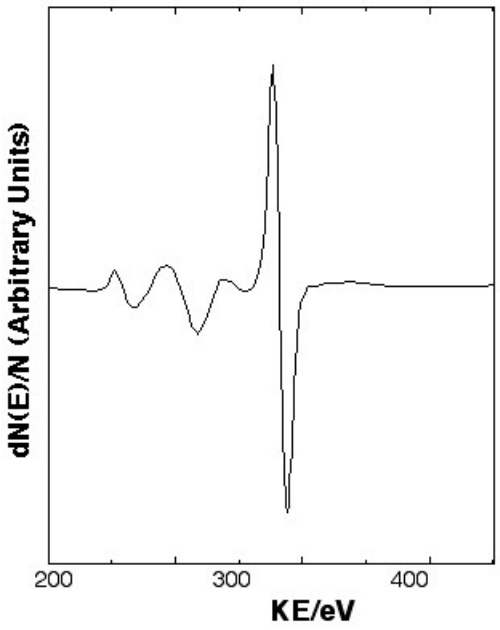

Figure 3*: Auger electron spectrum (AES) of a UHV-prepared clean and well-ordered Pd(111) electrode surface. Beam energy = 2 kV; beam current = 1.6* μA*.*

Case studies of molecular adsorption

A review of the literature reveals that studies with a bent on electrocatalysis are almost exclusively limited to Group VIIIB metals, especially platinum, since these materials interact strongly with a wide variety of organic compounds; the coinage metals interact only weakly with non-sulfur-containing molecules [1,2,57-59]. Studies discussed here are limited to polyatomic species adsorbed at single-crystal palladium electrode surfaces. The complexity of the subject compounds ranges from a diatomic species (carbon monoxide) to an anionic dihydroxysubstituted aromatic (hydroquinone sulfonate).

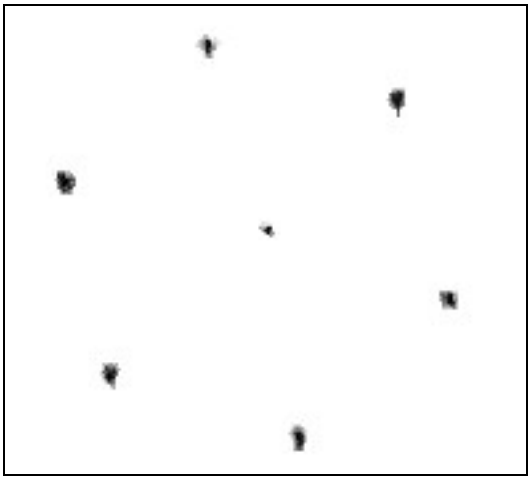

Figure 4*: LEED pattern of a clean and well-ordered Pd(111) electrode after a 180-second immersion in a 0.1 mM NaF/0.1 mM NaOH solution saturated with CO. The pattern is that for a Pd(111)-c(4x2)-CO adlattice. Electron beam energy = 60 eV; beam current = 2 μA.*

Carbon Monoxide

Chemisorption of CO from the gas phase onto well-ordered Pd(111) surfaces has been found to yield three adlattice structures [60-62]. At a surface coverage of 0.33 CO molecules per surface Pd atom ($\Theta_{CO} \equiv$ absolute surface coverage $\equiv \Gamma_{CO}/\Gamma_{Pd} = 0.33$, where Γ is the surface packing density in mol cm^{-2}), an ordered Pd(111)-($\sqrt{3}\times\sqrt{3}$)R30°-CO adlayer is formed. Dynamical LEED calculations [62] coupled with measurements of the C-O stretching frequency by infrared reflection-absorption spectroscopy (IRAS) [61] indicated that, at this coverage, CO is bonded solely at the three-fold hollow sites. At $\Theta_{CO} = 0.5$, a Pd(111)-c(4×2)-CO surface structure is produced in which the ($\sqrt{3}\times\sqrt{3}$) adlattice undergoes compression to allow for the coordination of additional CO molecules. Experimental and theoretical evidence has been invoked to suggest that the most probable molecular arrangement in the c(4×2) structure is one in which the CO molecules are chemisorbed on two-fold sites [63]. At still higher coverage, $\Theta_{CO} > 0.5$, IRAS measurements suggested the existence of CO chemisorbed on atop sites [61].

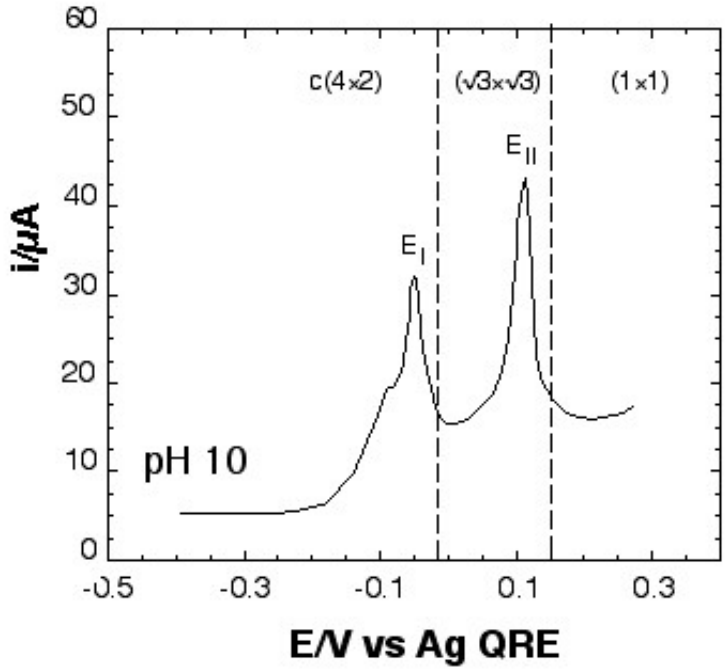

***Figure 5**: Current-potential curve for the anodic oxidation of CO chemisorbed on Pd(111), initially in the Pd(111)-c(4x2)-CO structure. The supporting electrolyte consisted of 0.1 mM NaF and 0.1 mM NaOH. The shoulder in peak I is due to polycrystalline-edge effects. Also indicated are the potential/coverage-dependent structures derived from the LEED patterns. The potential sweep rate was 2 mV/s.*

In comparison, immersion of a clean and *w*ell-ordered Pd(111) single-crystal electrode in a pH-10 solution saturated with CO yields only a Pd(111)-c(4×2)-CO adlattice [64]; this is as indicated by the LEED pattern shown in Figure 4. As with the gas-phase work, the CO molecules in this adlattice are thought to be coordinated at two-fold sites. The current-potential curve for the anodic oxidation of the Pd(111)-c(4×2)-CO adlattice, Figure 5, is characterized by two peaks, E_I = -0.05 V and E_{II} = 0.12 V. (As discussed elsewhere [64], the shoulder of peak I is attributed to oxidation of CO chemisorbed on atop sites at the polycrystalline edges of the single-crystal electrode.) The total charge under the areas of both peaks I and II is consistent with Θ_{CO} = 0.5, as would be expected for the c(4×2) structure. The relative areas are, respectively, about 40% and 60% of the total which indicates that the coverage of the CO layer that remains after the first oxidation peak is approximately 0.33; on a (111) substrate plane, this coverage would correspond to a Pd(111)-(√3×√3)R30°-CO structure, Figure 6. Subsequent oxidative desorption of the (√3×√3) CO adlayer at EII yields the (1×1) LEED pattern displayed in Figure 7.

The discussion thus far hints that CO oxidation at -0.05 V induces a c(4×2)-to-(√3×√3) *adlattice reconstruction*. Insights into this question can be obtained by examination of the c(4×2) and (√3×√3) LEED patterns individually and when superimposed; this is done in Figure 8 where it can be seen that the *simultaneous*

existence of c(4×2) and (√3×√3) structural domains would be manifested by four, rather than three, spots at the *fractional-index* positions for the pure c(4×2) adlattice. Such combined pattern, however, is clearly not substantiated by the actual LEED pattern shown in Figure 9. Hence, an essentially pure two-fold CO coordination is indicated for the c(4×2) layer, an assignment that is consistent with theoretical arguments [64].

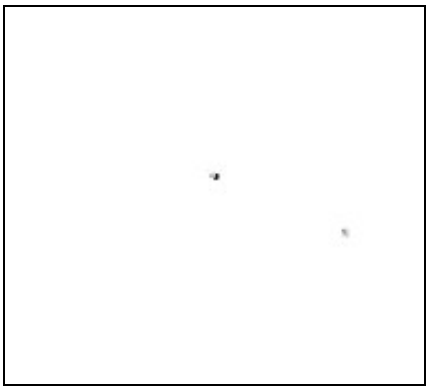

Figure 6*: LEED pattern obtained after the initial Pd(111)-c(4x2)-CO adlattice was emerged at potentials between -0.05 V (peak I) and 0.12 V (peak II). The new pattern is that for a Pd(111)-(√3x√3)R30°-CO adlayer. Experimental conditions were as in Figures 5 and 6.*

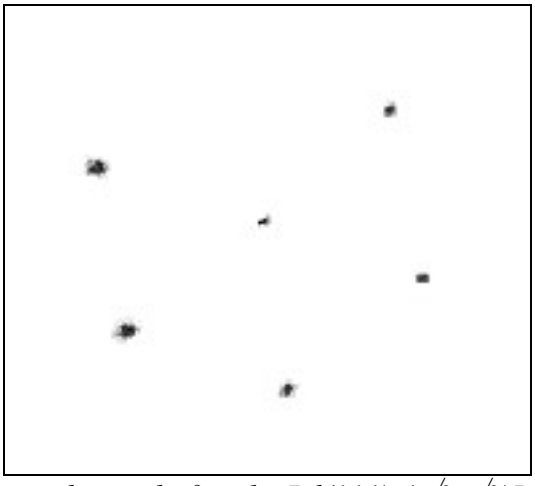

Figure 7*: LEED pattern obtained after the Pd(111)-(√3x√3)R30°-CO adlattice was emerged at potentials just past 0.12 V. The pattern is that for a clean and well-ordered Pd(111) surface. Experimental conditions were as in Figures 5 and 6.*

Based upon the voltammetric, coulometric, and LEED evidence, a sequence for the anodic oxidation of the Pd(111)-c(4×2)-CO adlattice in pH 10 NaF electrolyte can be suggested as shown in Figure 10.

The above-mentioned results point to the fact that a correlation exists between the ease of anodic oxidation, the binding site, and the extent of metal-to-ligand ð-electron back bonding. For example, CO adsorbed at three-fold hollow sites [($\sqrt{3}\times\sqrt{3}$) adlattice] is rather difficult to oxidize to CO_2 gas because the metal-CO bond is strong and the C≡O bond is weak. Comparatively, CO atop-site-bonded on the polycrystalline surface, is easy to oxidize since the metal-CO bond is weak and C≡O bond is strong. CO bonded at two-fold sites [c(4x2) structure] has properties intermediate between the two other cases. Such correlations between binding site and electrocatalytic reactivity parallel those established between binding site and ν_{CO} stretch frequency [61].

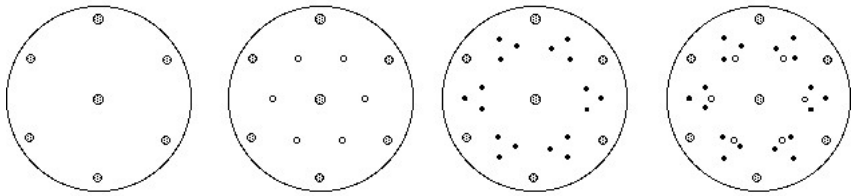

***Figure 8**: Idealized LEED patterns for Pd(111), Pd(111)-(√3x √3)R30°-CO, Pd(111)-c(4x2)-CO, and superimposed Pd(111)-(√3x √3)R30°-CO and Pd(111)-c(4x2)-CO adlattices.*

Hydroquinone and Benzoquinone

Figure 11 shows the HREEL spectrum of a Pd(100) surface after a 180-s exposure, at potentials within the double-layer region, to a 1 m*M* aqueous solution of tetrafluoroacetic acid (TFA). The spectrum is virtually identical to that of a freshly UHV-prepared surface; in other words, no TFA-derived species are chemically adsorbed on the Pd surface, a result previously reported for Pt surfaces [65].

The HREEL spectrum that results when the Pd(100) surface is emerged from an aqueous 1 m*M* TFA + 0.1 m*M* H2Q solution is shown in Figure 12. Three features in this spectrum warrant extra attention: (i) the absence of a peak at 3600 cm^{-1} which, by comparison with the gas-phase H_2Q spectrum [66], would have indicated an *in-plane* ν_{OH} stretch; (ii) the presence of peaks 2, 3 and 4 which, *if the adsorbed molecule retained its aromatic functionality*, would correspond to *in-plane* bending (δ_{CH}) and stretch (ν_{CC} and ν_{CH}) modes, respectively; [66, 67] and (iii) the appearance of peak 1 that could be attributed to an *out-of-plane* bending mode, γ_{CH}, [66, 67] the intensity of which is the highest of all observed peaks.

The absence of a ν_{OH} peak indicates either the absence of a phenolic O-H functional group and/or the imposition of a rigidly flat (η^6) adsorbed-aromatic orientation; in the latter configuration, the metal-surface dipole selection rule would render the O-H stretch HREELS-inactive [68]. However, if the dipole selection rule were to be strictly observed, peaks 2, 3 and 4 *(if those were actually in-plane aromatic-ring modes)* would likewise have been HREELS-inactive. Hence, the appearance of peaks 2 to 4 could be taken as an indication that the adsorbed molecule is *not* completely oriented parallel to the surface but is tilted, albeit only slightly. That the off parallel tilt is minimal

is evidenced by the out-of-plane peak being at least three times more intense than the in-plane modes. In the infrared spectrum of *unbound* hydroquinone [66], the reverse is true: the in-plane modes are actually three times more intense than the out-of-plane vibration. It should also be noted that, for gas-phase hydroquinone, the O-H peak is considerably more intense than the C-H stretch; yet the HREEL spectrum of chemisorbed H2Q shows only the C-H, without the O-H, peak. It may thus be postulated that, at least under the conditions of the present experiments, H2Q is *oxidatively chemisorbed* on Pd as benzoquinone (Q) in a slightly tilted η^6 orientation:

$$Pd + H_2Q_{(aq)} \rightarrow Pd\text{-}\eta^6\text{-}Q_{(ads)} + H_{2(g)} \quad (2)$$

An observed "rest-potential shift" in the *negative* direction upon chemisorption of H2Q provides evidence for an oxidative-chemisorption reaction. The $H_2Q_{(aq)}$ – to - $Q_{(ads)}$ chemisorption process has previously been reported for Pt [2, 4, 65].

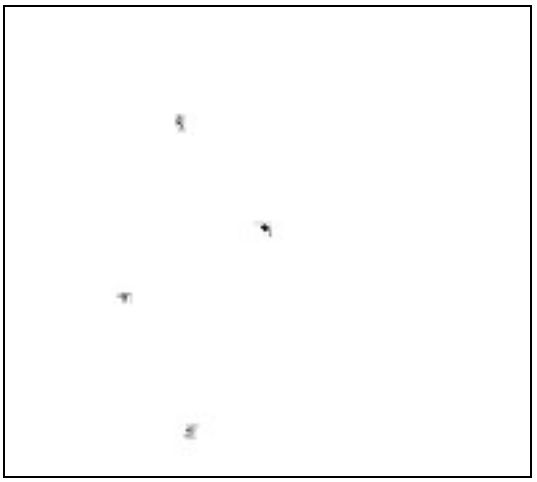

Figure 9*: LEED pattern of a Pd(111)-c(4x2)-CO adlattice at a different LEED setting than that in Figure 1 (beam energy = 32 eV; beam current = 3 μA) to isolate and magnify only the spots within the fractional-index positions. It is more convenient to compare this pattern with that for the superimposed (√3x√3) and c(4x2) structures in Figure 8.*

To investigate further the nature of the adsorbed species, identical HREELS-EC experiments were carried out using benzoquinone and Pd(111). It must first be mentioned that *no* rest-potential shift was observed upon chemisorption of Q, unlike the case for H_2Q just described above; that is, only simple chemisorption, neither oxidative nor reductive, occurs when Q interacts with Pd:

$$Pd + Q_{(aq)} \rightarrow Pd\text{-}\eta^6\text{-}Q_{(ads)} \quad (3)$$

The HREEL spectrum obtained after emersion of the Pd(111) surface from an aqueous 1 m*M* TFA + 0.1 m*M* Q solution is shown in Figure 13. It is clear that this spectrum is essentially identical to that shown in Figure 12. The close similarity between the two spectra indicates that the adsorbed species derived from aqueous H2Q is the same as that generated from aqueous Q. Such species is almost certainly benzoquinone, chemically bonded to the surface as in the organometallic complex, PtL2Q, where the ligand L is triphenylphosphine (PPh3) [69,70].

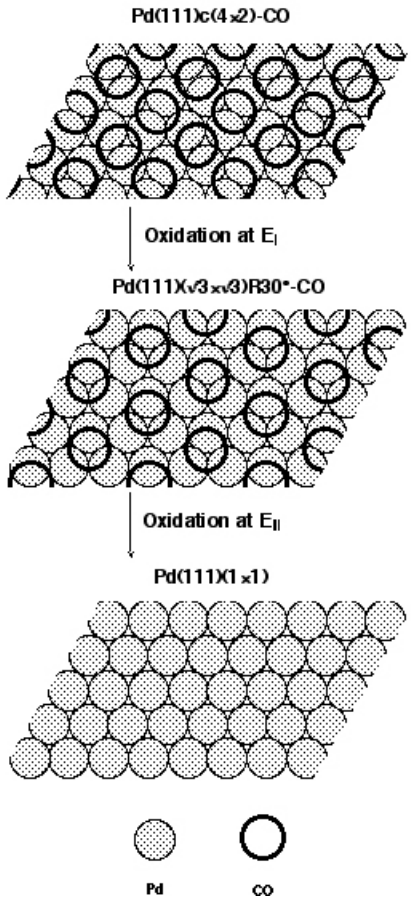

Figure 10*: Surface reconstructions of the Pd(111)-c(4x2)-CO adlattice brought about by step-wise anodic oxidation of the chemisorbed CO.*

Studies on the infrared spectra of PtL_2Q and the related organometallic complex, Zeise's salt, $PtL_2(C_2H_2)$, reveals that: (i) the frequency of the carbonyl C=O stretch can be lowered from 30 to 260 cm^{-1}, depending upon the metal and the position of the C=O functional groups, upon coordination of the quinone [69, 70]; and (ii) π-backbonding from the metal to the π* antibonding orbital of the olefin weakens the C=C bond in Zeise's complex by up to 140 cm^{-1}. When these coordination-induced frequency shifts are taken into account, it would not be unreasonable to consider the HREEL spectra in

Figures 12 and 13 to be due to a slightly tilted Pd-η^6-$Q_{(ads)}$ surface complex. In such a case, the frequency assignments would probably be as follows: peak 1 ~ γ_{CH}; peak 2 ~ ν_{CC} and/or δ_{CH}; peak 3 ~ ν_{CO}; and peak 4 ~ ν_{CH}. All but the (CH)-based peaks in the surface complex are *red-shifted* relative to those of the unbound Q. The small offparallel tilt allows for the activation of the in-plane modes.

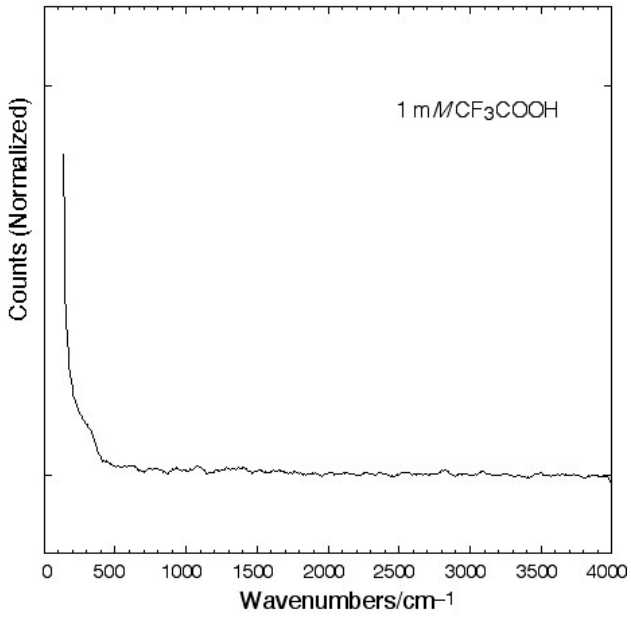

Figure 11*: High-resolution electron energy loss (HREEL) spectrum of a UHV-prepared Pd(100) surface after emersion from a 1 mM aqueous solution of trifluoroacetic acid (TFA).*

Support for the notion of a slightly tilted flat-oriented quinone can be gleaned from ECSTM experiments (Figure 14) in which a Pd(111) single-crystal facet was imaged while immersed in an aqueous solution of 0.01 m*M* H2Q in 0.05 *M* H2SO4. As can be seen from the high-resolution image, one of the *para*-oxygens in a quinone molecule is brighter (i.e., topographically higher) than the other. That is, the off-parallel tilt arises because one of the oxygens is pointed slightly upwards while the opposite oxygen is directed slightly downwards. It is not understood at this time why the quinone molecule does not adopt a strictly flat-oriented species, although the slight tilt may be related to packing efficiency. It should also be noted that, when chemisorbed onto the Pt-group metals, the benzene molecule is not rigidly flat but is bent into a boat-like surface structure [71].

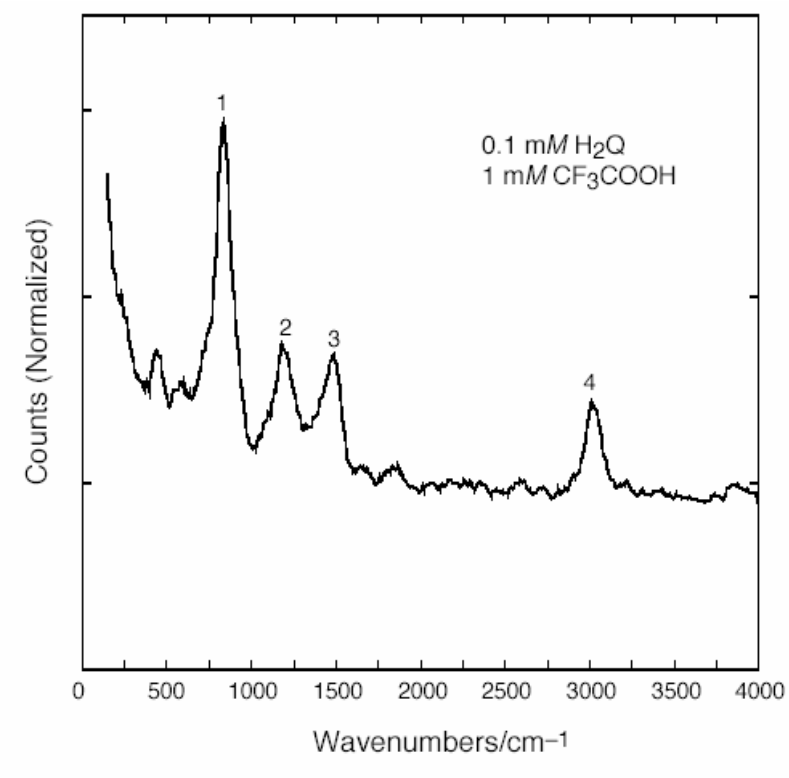

***Figure 12**: HREEL spectrum of a Pd(100) surface after emersion from a 0.1 mM aqueous solution of hydroquinone in 1 mM TFA.*

Electron Transfer Accompanied by Molecular Reorientation

We recently found that site-selective enhancement in the electron-transfer kinetics of the Q/H2Q redox couple occurs at iodine-pretreated platinum metals [72]. In particular, we found essentially Nernstian behavior in aqueous solutions, regardless of pH, when the surface contained chemisorbed iodine even at submonolayer coverages. In the absence of adsorbed iodine, the metal is covered with a full layer of chemisorbed Q, and a minimum in the electrode kinetics is observed at pH 4. In order to gain insight into this phenomenon, molecule-resolved EC-STM images were obtained of a well-ordered Pd(111)-(√3×√3)R30°-I surface in a 0.05 *M* H_2SO_4 solution that contained 10-4 *M* H_2Q at potentials where (i) only H_2Q is present in solution, and (ii) *partial* oxidation to Q has taken place.

Figure 15 shows the cyclic current-potential curve for the Q/H_2Q redox reaction at a Pd(111)-(√3×√3)R30°-I electrode surface in 0.05 *M* H_2SO_4. The arrows indicate the two potentials at which the EC-STM images described here were obtained. At E_1 (0.5 V), only H_2Q is present in solution; at E_2 (0.6 V), *partial* oxidation to Q takes place.

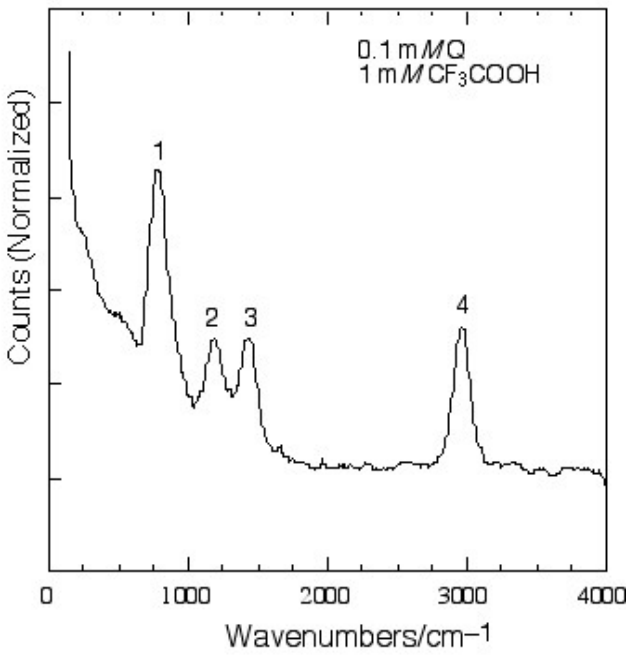

***Figure 13**: HREEL spectrum of a Pd(111) surface after emersion from a 0.1 mM aqueous solution of benzoquinone in 1 mM TFA.*

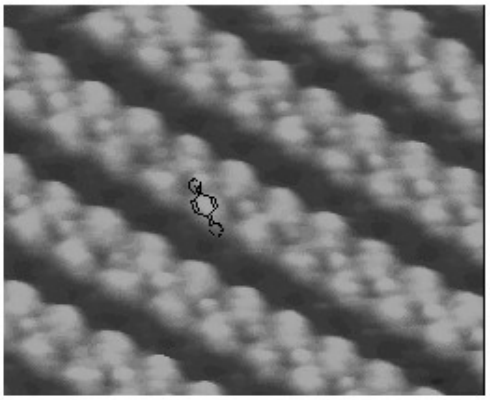

***Figure 14**: High-resolution electrochemical scanning tunneling microscope image of a Pd(111) facet immersed in a 0.01 mM aqueous solution of hydroquinone in 0.05 M H_2SO_4. Bias voltage = 200 mV. Tunneling current = 2 0 nA.*

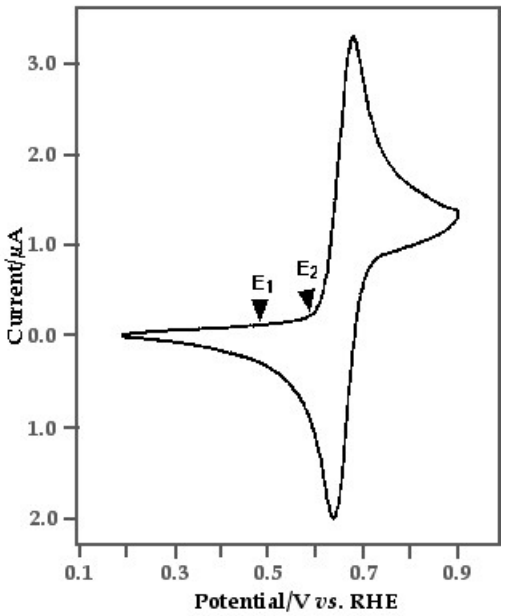

***Figure 15**: Steady-state cyclic voltammogram of Pd(111)-(√3x √3)R30°-I in a 0.05 M H_2SO_4 that contained 10-4 M hydroquinone (H_2Q). The potential scan rate was 50 mV/s.*

Figure 16 shows the EC-STM image at E1 where an ordered adlattice is produced. It is important to emphasize that, since the Pd surface has been passivated by the chemisorbed I layer, *no direct Pd-organic interactions are possible*; that is, the organic monolayer self-assembles in a well-ordered structure primarily due to favorable adsorbate-adsorbate interactions. It is evident from the EC-STM image in Figure 16 that the physisorbed H2Q molecules are oriented parallel to the surface; the adlayer structure is (√21×√21)R10.9°-η^6-H_2Q.

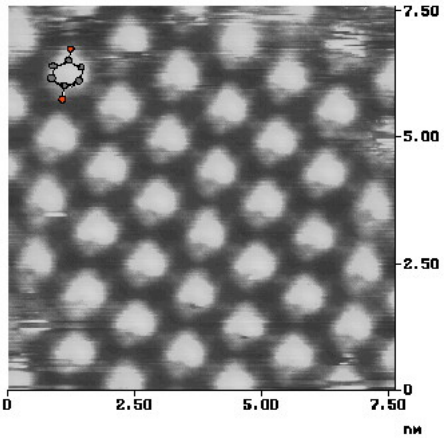

***Figure 16**: Molecule-resolved EC-STM image of Pd(111)-(√3x √3)R30°-I in a 0.05 M H_2SO_4 solution that contained 10-4 M H2Q at E_1 (0.5 V). Bias voltage = 200 mV. Tunneling current = 2 nA.*

When the potential is stepped to E_2, the EC-STM image shown in Figure 17 was obtained. Three features are noteworthy: (i) as at E1, an ordered self-assembled adlayer is generated; (ii) a two-dimensional structure identical to that at E1 can be derived, but (iii) the unit mesh coverage is twice as large. The doubling of the coverage, as well as the molecular dimensions extracted from the EC-STM image, indicates a molecular reorientation, after *partial* oxidation, of the self-assembled layer in which the initially flat-adsorbed molecules adopt a vertical (edgewise) orientation. On closer scrutiny, it can be noted that the vertically-oriented species are *not* structurally identical: One is discernibly more elongated than the other; in addition, it can also be observed that these non-identical species are arranged alternately. Because, at E_2, a fraction of the H_2Q has been converted to Q, it is not unreasonable to associate the (slightly) longer species with H_2Q and the (slightly) shorter molecules with Q. This onedimensional, alternating Q-H_2Q arrangement is very similar to what exists in the crystal structure of *quinhydrone*, an equimolar mixture of Q and H_2Q (*cf.*, Figure 18) [73]. The self-assembled adlattice in Figure 24 can thus be designated as $(\sqrt{21}\times\sqrt{21})R10.9°$-$\eta^2$-QH, where QH represents *quinhydrone*.

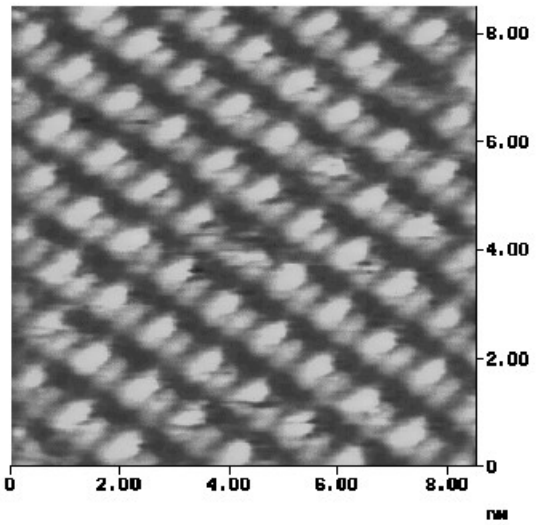

Figure 17*: Molecule-resolved EC-STM image of Pd(111)-(* $\sqrt{3}$*x* $\sqrt{3}$*)R30°-I in a 0.05 M* H_2SO_4 *solution that contained 10-4 M* H_2Q *at* E_2 *(0.6 V).*

When the potential is reverted from E_2 back to E_1, a structure identical to that shown in Figure 16 is obtained. This result provides evidence that the (partial) oxidation-induced η^6-to-η^2 adsorbed-molecule reorientation is reversible. Such reorientation appears to be driven by attractive Q-H_2Q "face-to-face" interactions. Hence, at more positive potentials where only Q would exist in solution, an ordered self-assembled layer of η^6-oriented Q molecules would be anticipated. Unfortunately, at those potentials, several interfacial processes occur (e.g., larger faradaic currents, higher organic adlayer coverages, and $I_{(ads)}$-catalyzed dissolution of Pd [74]) that prevent the observation of noise-free EC-STM images.

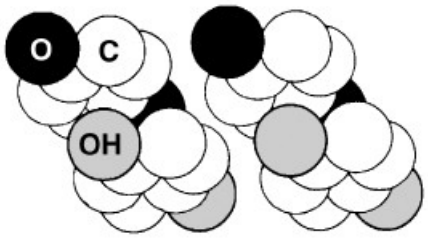

***Figure 18**: The crystal structure of quinhydrone, an equimolar mixture of Q and H_2Q [74].*

Hydroquinonesulfonate

Figure 19(A) shows the HREEL spectrum of a Pd(111) surface emerged from an aqueous 1 m*M* TFA + 0.1 m*M* hydroquionesulfonate (HQS) solution. Three important features in the spectrum should be pointed out. The first is the absence of a peak at *ca.* 3600 cm^{-1} which, based upon the infrared spectrum of bulk diphenolic species [74], would have indicated an O-H stretch (ν_{OH}). The second is the presence of the peaks at 545, 634 and 1260 cm^{-1}; respectively, these correspond to the S-O ($\nu_{S\text{-}O}$), C-S (ν_{CS}) and S=O ($\nu_{S=O}$) stretch modes of the sulfonate group. The third is the presence of the peaks at 810, 1466 and 3007 cm^{-1} which, if the adsorbed molecule retained its aromatic functionality, would correspond, respectively, to one out-of-plane bending mode (γ_{CH}) and two in-plane stretch modes ($\nu_{C=C}$ and ν_{CH}).

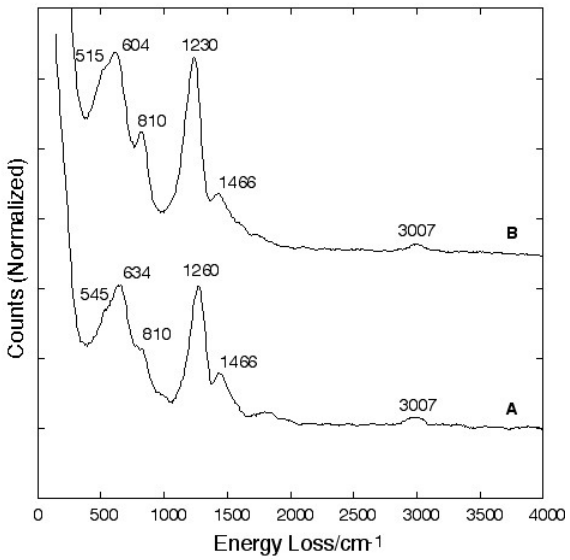

***Figure 19**: HREEL spectrum of a UHV-prepared Pd(111) surface. A: After emersion from an aqueous 1 mM TFA + 0.1 mM HQS solution. B: After emersion from an aqueous 1 mM TFA + 100 mM HQS solution. The crystal was rinsed with HQS-free 1 mM TFA solution prior to surface analysis. Experimental conditions: incident beam energy = 4 eV. Incidence and detection angles = 62° from the surface normal. Beam current = 100 pA.*

Molecular models suggest that chemisorption of HQS via its p-electron system would result in a tilted-flat orientation because of steric hindrance by the bulky sulfonate group; the tilt angle was *estimated* to be 20°. Thus, for this adsorbate, the metal-surface dipole selection rule [76], with respect to the in-plane modes, may not be strictly enforceable. That the off-parallel tilt is minimal is evidenced by fact that the *out-of-plane* bend, γ_{CH}, is at least three times more intense than the *in-plane* stretch, ν_{CH}. An important consequence of the inapplicability of the metal-surface dipole selection rule is that the absence of a ν_{OH} peak can be regarded as an indication of the absence of a phenolic O-H functional group.

The postulate is thus that, at least under the conditions of the present experiments, HQS is oxidatively chemisorbed on Pd(111) as benzoquinone sulfonate (BQS) in a slightly tilted η^6 orientation:

$$Pd + C_6H_3(OH)_2SO_3^-{}_{(aq)} \rightarrow Pd\text{-}\eta^6\text{-}\ C_6H_3O_2SO_3^-{}_{(ads)} + H_2(g) \qquad (4)$$

where the $C_6H_3(OH)_2SO_3^-$ and $C_6H_3O_2SO_3^-$ are the reduced (HQS) and oxidized (BQS) forms, respectively. The oxidative chemisorption reaction (3) is identical to that for hydroquinone described by Equation (2) above.

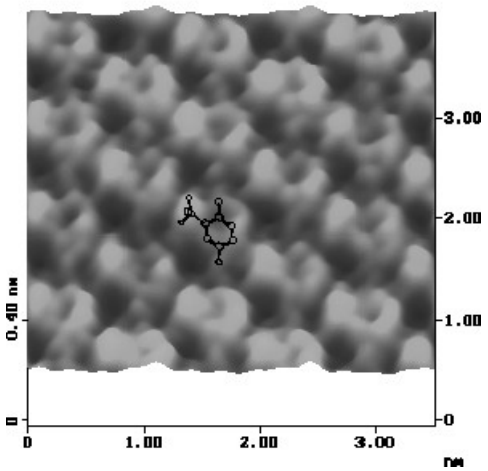

Figure 20*: High-resolution EC-STM image of a Pd(111) single-crystal facet immersed in an aqueous 0.1 mM HQS + 0.1 M $HClO_4$ solution. Experimental conditions: bias potential = 100 mV; tunneling current = 10 nA.*

If the adsorbed molecule were in the quinone form, one may expect a peak at *ca.* 1700 cm^{-1}, the frequency that corresponds to the in-plane C=O ($\nu_{C=O}$) stretch [74]. The absence of this peak in Figure 19(A) may be rationalized in terms of what is known from the organometallic chemistry literature. Previous infrared spectroscopic studies of the platinum complexes of quinone and ethylene have shown that $\nu_{C=O}$ and $\nu_{C=C}$ are red-shifted, up to 260 and 140 cm^{-1} respectively, relative to those for the uncomplexed molecules. When such coordination-induced frequency shifts are taken into account, it would not be unreasonable to consider the peak at 1466 cm^{-1}, originally assigned to a C=C stretch, to arise from a C=O stretch; in the same vein, the peak at 1260 cm^{-1} can be

attributed to an overlap of the S=O and the (red-shifted) C=C stretch modes. The complete frequency assignments have been reported elsewhere [75].

To determine if the mode of chemisorption of HQS is dependent upon its concentration in the aqueous phase, an HREEL spectrum was obtained for Pd(111) exposed to 100 m*M* HQS in 1 m*M* TFA (but rinsed with 0.1 m*M* HQS prior to the HREELS experiments); the result is displayed in Figure 19(B). It is evident that the spectral features are identical to those for the adlayer formed from 0.1 m*M* HQS [Figure 19(A)]; such result points to the conclusion that the mode of chemisorption of HQS on Pd(111) is *unaltered* by a 103-fold increase in the aqueous solution concentration of the adsorbate. The slight increase in peak intensities is almost certainly due to a slight increase in coverage (i.e., slightly denser packing) rather than to a flat-to-vertical reorientation; the latter would have resulted in a significantly larger increase in surface coverage.

Support for the notion of a slightly tilted η^6-oriented BQS was obtained from EC-STM experiments with a Pd(111) single-crystal facet immersed in an aqueous solution of 0.1 m*M* HQS + 0.1 m*M* $HClO_4$. The high-resolution image, shown in Figure 20, reveals that the BQS adlayer- is well-ordered and that the adsorbed molecules, in accordance with molecular models, are not oriented completely parallel to the surface but are slightly tilted. It is remarkable that both the sulfonate and quinonoid moieties are discernible in the image. For example, it can be seen that one of the oxygens in the sulfonate group is brighter than the other two, a result that can be viewed as one oxygen atom pointed upwards with the other two directed downwards.

The EC-STM experiments were unable to image the counter-cations associated with the anionic sulfonate group. This is most likely because the counter-cations are not held rigidly within, but are quite mobile atop, the organic adlayer; in such a case, the counter-ions can be easily moved aside by the STM tip.

Acknowledgments

Acknowledgment is made to the National Science Foundation (CHE-9703521) and to the Robert A. Welch Foundation for support of this research.

References

[1] Soriaga, M.P. In *Frontiers of Electrochemistry. Structure of Electrified Interfaces.* Ross, P. N.; Lipkowski, J. Eds.; VCH Publishers: New York, NY (**1993**).
[2] Hubbard, A.T. *Chem. Rev.* **1988**, *88*, 633.
[3] Salaita, G.N.; Hubbard, A.T. In *Molecular Design of Electrode Surfaces.* Murray, R.W. Ed.; John Wiley: New York, **1989**.
[4] Damaskin, B.B.; Petrii,O.A.; Batrakov. V.V. *Adsorption of Organic Compounds on Electrodes.* Plenum Press: New York, **1971**.
[5] Snell, R.D.; Keenan, A.G. *Chem. Soc. Rev.* **1979**, *8*, 259.
[6] Stickney, J.L.; Soriaga, M.P.; Hubbard, A.T.; Anderson, S.E. *J. Electroanal. Chem.* **1981**, *125*, 73.
[7] Michelhaugh, S.L.; Bhardwaj, C., Cali, G.J.; Bravo, B.G.; Bothwell, M.E.; Berry, G.M.; Soriaga, M.P. *Corrosion.* **1991**, *47*, 322.

[8] Yeager, E.; Kuta, J. In *Physical Chemistry: An Advanced Treatise. IXA* Eyring, H.; Henderson, D.; Jost, W. Eds. Academic Press: New York, **1970**.
[9] Bard, A.J.; Faulkner, L.R. *Electrochemical Methods*. John Wiley: New York, **1980**.
[10] Soriaga, M.P.; Hubbard, A.T. *J. Electroanal. Chem.* **1984**, *167*, 79.
[11] White, R.E.; Bockris, J.O'M.; Conway, B.E.; Yeager, E. Eds. *Comprehensive Treatise of Electrochemistry. VIII.* Plenum Press: New York, **1984**.
[12] Bard, A.J.; Abruña, H.D.; Chidsey, C.E.; Faulkner, L.R.; Feldberg, S.; Itaya, K.; Melroy, O.; Murray, R.W.; Porter, M.D.; Soriaga, M.P.; White, H.S. *J. Phys. Chem.* **1993**, *97*, 7147.
[13] Furtak, T.E.; Kliewer, K.L.; Lynch, D.W. Eds. *Non-Traditional Approaches to the Study of the Solid-Electrolyte Interface.* North-Holland: Amsterdam, **1980**.
[14] Hansen, W.N.; Kolb, D.M.; Lynch, D.W. Eds. *Electronic and Molecular Structure of Electrode-Electrolyte Interfaces*. Elsevier: Amsterdam, **1983**.
[15] Faulkner, L.R. *In Situ Characterization of Electrochemical Processes.* National Academy Press: Washington, D. C., **1987**.
[16] Soriaga, M.P. Ed. *Electrochemical Surface Science: Molecular Phenomena at Electrode Surfaces.* American Chemical Society: Washington, D. C., **1988.**
[17] Hubbard, A.T. *Accts. Chem. Res*. **1980**, *13*, 177.
[18] Ross, P.N. In *Chemistry and Physics of Solid Surfaces*, Vaneslow, R.; Howe, R. Eds. Springer-Verlag: New York, **1982**.
[19] Yeager, E.; Homa, A.; Cahan, B.D.; Scherson, D. *J. Vac. Sci. Technol.* **1982**, *20*, 628.
[20] Kolb., D.M. *Z. Phys. Chem. N. F.* **1987**, *154*, 179.
[21] Somorjai, G.A. *Chemistry in Two Dimensions: Surfaces.* Cornell University Press: New York, **1981**.
[22] Ertl. G.; Kuppers, J. *Low Energy Electrons and Surface Chemistry.* VCH Publishers: New York, **1985**.
[23] Woodruff, D.P.; Delchar, T.A. *Modern Techniques of Surface Science.* Cambridge University Press: New York, **1986**.
[24] Van Hove, M.A.; Wang, S.W.; Ogletree, D.F.; Somorjai, G.A. *Adv. Quant. Chem.* **1989**, *20*, 1.
[25] Rhodin, T.H.; Ertl, G. Eds. *The Nature of the Surface Chemical Bond.* North-Holland Publishing: New York, **1979**.
[26] Muetterties, E. L. *Bull. Chim. Belg.* **1975**, *84*, 959.
[27] Muetterties, E.L. *Bull. Chim. Belg.* **1976**, *85*, 451.
[28] Shustorovich, E.; Baetzold, R.C.; Muetterties, E.L. *J. Phys. Chem.* **1983**, *87*, 1100.
[29] Hoffman, R. *Solids and Surfaces: A Chemist's View of Bonding in Extended Structures*. VCH Publishers: New York, **1988**.
[30] Albert, M.R.; Yates, J.T. *A Surface Scientist's Guide to Organometallic Chemistry.* American Chemical Society: Washington, D. C., **1987**.
[31] Soriaga, M.P.; Binamira-Soriaga, E.; Hubbard, A.T.; Benziger, J.B.; Pang. K.W.P. *Inorg. Chem.* **1985**, *24*, 65.
[32] Lewis, G.J.; Roth, J.D.; Montag, R.A.; Safford, L.K.; Gao, X.; Chang, S.C.; Dahl, L.F.; Weaver, M.J. *J. Am. Chem. Soc.* **1990**, *112*, 2831.

[33] Schardt, B.C.; Stickney, J.L.; Stern, D.A.; Frank, D.G.; Katekaru, J.Y.; Rosasco, S.D.; Salaita, G.N.; Soriaga, M.P.; Hubbard, A.T. *Inorg. Chem*. **1985**, *24*, 1419.
[34] Soriaga., M.P. *Chem. Rev*. **1990**, *90*, 771.
[35] Wieckowski, A. In *Modern Aspects of Electrochemistry. XXI.* White, R.E.; Bockris, J.O'M.; Conway, B.E. Eds. Plenum Press: New York, NY (**1990**).
[36] Hartley, F.R. *The Chemistry of Platinum and Palladium.* Wiley: New York, NY (**1973**).
[37] Belluco, U. *Organometallic and Corodination Chemistry of Platinum.*" Academic Press: New York, NY (**1974**).
[38] Halpern, J.; Kemp, A.L.W. *J. Am. Chem. Soc.* **1966**, *58*, 5147.
[39] Soriaga, M.P. *Prog. Surf. Sci*. **1992**, *39*, 325.
[40] Soriaga, M.P.; Stickney, J.L. In *Modern Techniques in Electroanalysis*. Vanysek, P. Ed. Wiley: New York, NY (**1996**).
[41] Soriaga, M.P.; Harrington, D.A.; Stickney, J.L.; Wieckowski, A. In *Modern Aspects of Electrochemistry. XXVIII.* Conway, B.E.; Bockris, J.O'M.; White, R.E. Eds. Plenum Press: New York, NY (**1996**).
[42] Will, F.G. *J. Electrochem. Soc.* **1965**, *112*, 451.
[43] Hubbard, A.T.; Ishikawa, R.M.; Katekaru, J. *J. Electroanal. Chem.* **1978**, *86*, 271.
[44] Solomun, T.; Schardt, B.C.; Rosasco, S.D.; Wieckowski, A.; Stickney, J.L.; Hubbard, A.T. *J. Electroanal. Chem*. **1984**, *176*, 309.
[45] Adzic, R.R.; Tripkovic, A.V.; Vesovic, V.B. *J. Electroanal. Chem*. **1986**, *204*, 329.
[46] Rodes, A.; Orts, J.M.; Feliu, J.M.; Aldaz, A.; Clavilier, J. *J. Electroanal. Chem*. **1990**, *281*, 199.
[47] Wood, E.A. *Crystal Orientation Manual*. Columbia University Press: New York, **1963**.
[48] Clavilier, J. *J. Electroanal. Chem*. **1980**, *107*, 205.
[49] Aberdam, D.; Durand, R.; Faure, R.; El-Omar, F. *Surface Sci.* **1986**, *171*, 303.
[50] Clavilier, J. In *Electrochemical Surface Science: Molecular Phenomena at Electrode Surfaces.* M.P. Soriaga, Ed.; ACS Books: Washington, D.C., **1988**.
[51] Kim, Y.-G.; Soriaga, M.P. *J. Phys. Chem. B*. **1998**, *102*, 6188.
[52] Kim, Y.-G.; Soriaga, J.B.; Vigh, Gy.; Soriaga, M.P. *J. Coll. Interf. Sci*. **2000**, *227*, 505.
[53] Kim, Y.-G; Soriaga, M.P. In *Interfacial Electrochemistry*. Wieckowski, A. Ed. Marcel Dekker: New York, NY (**1999**).
[54] Hansen, W.N. *J. Electroanal. Chem.* **1983**, *150*, 133.
[55] Hofman, O.; Doblhofer, K.; Gerischer, H. *J. Electroanal. Chem*. **1984**, *161*, 337.
[56] Pemberton, J.E.; Sobocinksi, R.L.; Bryant, M.A. *J. Am. Chem. Soc*. **1990**, *112*, 6177.
[57] Campion, A. In *Vibrational Spectroscopy of Molecules on Surfaces.* Yates, J.T; Madey, T.E. Eds. Plenum: New York, NY (**1987**).
[58] Dubois, L.J.; Nuzzo, R.G. *Ann. Rev. Phys. Chem*. **1992**, *43*, 439.
[59] Bard, A.J. *Integrated Chemical Systems. A Chemical Approach to Nanotechnology.* Academic Press: Boston, MA (**1994**)
[60] Conrad, H.; Ertl, G.; Kuppers. J. *Surf. Sci.* **1978**, *187*, 372.
[61] Bradshaw, A. M. *Surf. Sci*. **1978**, *72*, 513.

[62] Ohtani, H.; Hove, M. A.; Somorjai, G. A. *Surf. Sci.* **1987**, *187*, 372.
[63] Wong, Y.T.; Hoffmann, R. *J. Phys. Chem*. **1991**, *95*, 859.
[64] Berry, G.M.; Bothwell, M.E; Michelhaugh, S.L; McBride; J.R; Soriaga, M.P. *J. Chim. Phys.* **1991**, *88*, 1591.
[65] Stern, D.A.; Wellner, E.; Walton, N.; Zapien, D.C.; Salaita, G.N.; Lu, F.; Laguren-Davidson, L.; Batina, N.; Frank, D.G.; Hubbard, A.T. *J. Am. Chem. Soc.* **1998**, *110*, 4885.
[66] Shimanouchi. T. *Standard Reference Database.* NIST: Washington, DC (**1998**).
[67] Kesmodel, L.K. In *Surface Imaging and Visualization.* Hubbard, A. T. Ed. CRC Press: Boca Raton, FL (**1995**).
[68] Ibach, H.; Mills. D.A. *Electron Energy Loss Spectroscopy.* Academic, New York (**1982**).
[69] Belluco, U. *Organometallic and Coordination Chemistry of Platinum.* Academic Press: New York, NY (**1974**).
[70] Hartley, F.R. *The Chemistry of Platinum and Palladium.* Wiley: New York, NY (**1973**).
[71]. Somorjai, G.A. *J. Phys. Chem.* **1990**, *94*, 1013.
[72] Michelhaugh, S.L.; Carrasquillo, A.; Soriaga, M.P. *J. Electroanal. Chem.* **1991**, *319*, 387.
[73] Wyckoff, R.W.G. *Molecular Structures.* John Wiley: New York, NY (**1963**).
[74] Sashikata, K.; Matsui, Y.; Itaya, K.; Soriaga, M.P. *J. Phys. Chem.* **1996**, *100*, 20027.
[75] Soto, J.E.; Kim, Y.-G.; Chen, X.; Park, Y.-S.; Soriaga, M.P. *J. Electroanal. Chem*. **2001**, *500*, 374.